

AD-A260 029



2

PL-TR-92-2246

**THE LIQUID CRYSTAL POLARIMETER
FOR SOLID-STATE IMAGING
OF SOLAR VECTOR MAGNETIC FIELDS**

Laurence J. November
Lawrence M. Wilkins

DTIC
ELECTE
DEC 11 1992
S C D

National Solar Observatory
National Optical Astronomy Observatories
Sunspot, NM 88349

28 September 1992

Final Report
01 October 1988 to 30 September 1992

92-31254



20pg

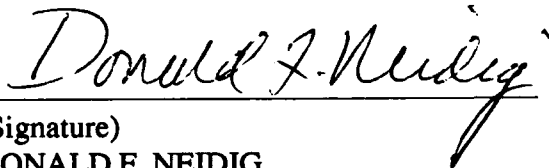
APPROVED FOR PUBLIC RELEASE; DISTRIBUTION UNLIMITED



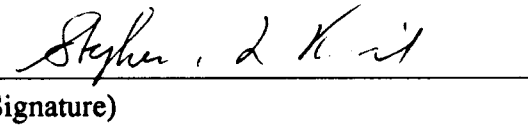
PHILLIPS LABORATORY
Directorate of Geophysics
AIR FORCE MATERIEL COMMAND
HANSCOM AIR FORCE BASE, MA 01731-5000

92 12 10 018

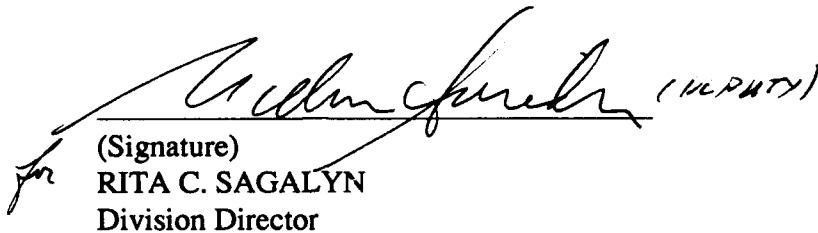
This technical report has been reviewed and is approved for publication.


(Signature)

DONALD F. NEIDIG
Contract Manager


(Signature)

STEPHEN L. KEIL
Branch Chief


(Signature)
RITA C. SAGALYN
Division Director

This document has been reviewed by the ESD Public Affairs Office (PA) and is releasable to the National Technical Information Service (NTIS).

Qualified requesters may obtain additional copies from the Defense Technical Information Center. All others should apply to the National Technical Information Service.

If your address has changed, or if you wish to be removed from the mailing list, or if the addressee is no longer employed by your organization, please notify PL/TSI, Hanscom AFB, MA 01731-5000. This will assist us in maintaining a current mailing list.

Do not return copies of this report unless contractual obligations or notices on a specific document requires that it be returned.

REPORT DOCUMENTATION PAGE			Form Approved OMB No. 0704-0188	
<small>Public reporting burden for this collection of information is estimated to average 1 hour per response, including the time for reviewing instructions, searching existing data sources, gathering and maintaining the data needed, and completing and reviewing the collection of information. Send comments regarding this burden estimate or any other aspect of this collection of information, including suggestions for reducing this burden, to Washington Headquarters Services, Directorate for Information Operations and Reports, 1215 Jefferson Davis Highway, Suite 1204, Arlington, VA 22202-4302, and to the Office of Management and Budget, Paperwork Reduction Project (0704-0188), Washington, DC 20503.</small>				
1. AGENCY USE ONLY (Leave blank)		2. REPORT DATE 28 September 1992		3. REPORT TYPE AND DATES COVERED Final 01 Oct 88 to 30 Sep 92
4. TITLE AND SUBTITLE The Liquid Crystal Polarimeter for Solid-State Imaging of Solar Vector Magnetic Fields			5. FUNDING NUMBERS PE 61101F PR ILIR TA 9C WUAA	
6. AUTHOR(S) Laurence J. November Lawrence M. Wilkins			Project Order GLH9-6028	
7. PERFORMING ORGANIZATION NAME(S) AND ADDRESS(ES) National Solar Observatory National Optical Astronomy Observatories Sunspot, NM 88349			8. PERFORMING ORGANIZATION REPORT NUMBER	
9. SPONSORING / MONITORING AGENCY NAME(S) AND ADDRESS(ES) Phillips Laboratory Hanscom AFB, MA 01731-5000 Contract Manager: Donald Neidig/GPSS			10. SPONSORING / MONITORING AGENCY REPORT NUMBER PL-TR-92-2246	
11. SUPPLEMENTARY NOTES This research was supported by the AF Inhouse Laboratory Independent Research Fund.				
12a. DISTRIBUTION / AVAILABILITY STATEMENT APPROVED FOR PUBLIC RELEASE; DISTRIBUTION UNLIMITED			12b. DISTRIBUTION CODE	
13. ABSTRACT (Maximum 200 words) The Liquid Crystal Polarimeter (LCP) is a low-voltage complete Stokes polarimeter and spectral analyzer designed for measuring solar vector magnetic fields. The polarimeter consists of polarization and spectral analyzer sections each containing multiple commercially available nematic and ferro-electric liquid crystals that are modulated in phase at up to 31.5 kHz frequency. Used in conjunction with a Lyot birefringent filter and 2 ccds, the system provides a complete polarization/spectral measurement for solid-state direct imaging of the vector magnetic flux, Doppler velocity, intensity, and line width in a spectral line. Simultaneous 2 ccd imaging gives reduced atmospheric seeing systematics, and automatic ccd gain and dark-current correction. The liquid-crystal design provides a considerable simplification to previous designs with greatly improved speed, sensitivity, reliability, and accuracy. The system is used with a universally tunable Lyot filter (of conventional rotating-element design) to provide sequential observations in a number of solar lines to permit calibration of field strength and measurements as a function of height in the solar atmosphere. An example vector magnetogram is shown as a proof of concept.				
14. SUBJECT TERMS Liquid Crystal, Stokes Polarimeter, Solar Vector Magnetic Fields, Birefringent Filter			15. NUMBER OF PAGES 20	
			16. PRICE CODE	
17. SECURITY CLASSIFICATION OF REPORT UNCLASSIFIED	18. SECURITY CLASSIFICATION OF THIS PAGE UNCLASSIFIED	19. SECURITY CLASSIFICATION OF ABSTRACT UNCLASSIFIED	20. LIMITATION OF ABSTRACT SAR	

CONTENTS

1. INTRODUCTION	1
2. DESIGN CONCEPT OF POLARIMETER/SPECTRAL ANALYZER	2
3. EXPERIMENTAL RESULTS	8
4. IN-SITU CALIBRATION	13
5. CONCLUSION	14
REFERENCES	15

DTIC QUALITY INSPECTED

Accession For	
NTIS GR&I	<input checked="" type="checkbox"/>
DTIC TAB	<input type="checkbox"/>
Unannounced	<input type="checkbox"/>
Justification	
By	
Distribution/	
Availability Codes	
Avail and/or	
Dist	Special
A-1	

1. INTRODUCTION

Predictions for solar activity and its subsequent effects on DoD systems rely heavily on monochromatic imaging in several wavelengths with polarimetric measurements for observing the solar magnetic-field evolution. Such data are presently acquired by the AWS/SEON system and are transmitted to the Space Environment Services Center which is jointly operated by NOAA and the USAF Space Forecast Center. Other magnetograph systems are operated by Big Bear Solar Observatory, by the NASA Marshall Facility in Huntsville, and at the Mees Solar Observatory at Haliakala in Hawaii. All of these systems are based upon conventional Lyot birefringent filters which are mechanically tuned or sample only one point in the line or use high voltage KD*Ps. It is well known that systems with moving optical parts are slow and show image alignment and systematic quality differences with orientation change. Measurements from a single spectral point are subject to ambiguous interpretation of magnetic field with velocity and line strength. High-voltage modulators are difficult to maintain and control reliably. With the availability of new liquid-crystal polarization retarders it is possible to simplify the magnetograph design with low-voltage solid-state optical systems having improved speed, sensitivity, reliability, and accuracy. This study presents the first magnetic-field measurements made with a polarimeter based upon liquid-crystal technology.

Liquid crystal devices consist of a cholesteric fluid sandwiched between two optically flat pieces of glass which are coated with a thin, transparent, electrically conducting layer. Two basically different types are available based upon nematic and smectic cholesteric fluids, respectively. Nematic devices provide low-voltage variable tuning retarders with relatively slow tuning properties (5 milliseconds). Smectic devices are fixed retarders which have two low-voltage rotational states for fast state switching (.05 milliseconds). Smectic devices called "ferroelectric" liquid crystals are commercially available from Displaytech Inc. which are nearly achromatic half-wave retarders in the visible. The electrical switching between the states is equivalent in its polarization effect to rotating the device through 45° . Programmable tuning with precise timing is obtained with low-voltage control circuitry with modulation frequencies set with computer controller. The commercial materials used were all of excellent optical quality ($\lambda/10$). The ferroelectrics exhibit high transmittance (96%) and very good uniformity ($< 1\%$ retardance variation over the field of view). The nematics used in the present proof of concept were acquired from Meadowlark optics. They have good transmittance (93%) and fair uniformity ($\sim 5\%$ variation within the specified clear aperture).

A design idea well suited for a solid-state magnetograph has been available based upon the natural passband characteristics of Lyot birefringent filters. A stack of liquid crystal elements is arranged for selecting and modulating the polarization state input into a Lyot filter while a stack is modulated in phase as a spectral discriminator after the filter. The two sections, the polarization and spectral analyzer sections, comprise the LCP. The principle was used successfully with KD*P crystals to provide high-resolution longitudinal magnetograms (November 1984). Liquid crystals give the same possibility for vector magnetograms with a simpler and more reliable hardware system. The principle of operation is described in Section 2.

Optimally, the Lyot filter passband should be the width of the solar line. The advan-

tage of using a relatively large passband is the high signal. The polarized signal increases in proportion to the total polarized light but the noise increases only in proportion to the square root of the total integrated intensity. The light levels are high at the normal image scale of the National Solar Observatory/Sacramento Peak (NSO/SP) Vacuum Tower Telescope (VTT) provides adequate light for video operation. An example vector magnetogram obtained using this concept is shown in Section 3 using normal ccds with about 2 seconds readout time per exposure or a total of 30 seconds for the vector magnetogram. It should be possible to obtain vector magnetograms having this signal to noise in about 1/2 second with video. The LCP is an inherently sensitive design and with proper readout electronics should be ideally suited to study weak vector fields, fast transient phenomena, electric fields using the Stark effect, or particle-beam impact polarization effects using the same design concept presented here.

One of the major difficulties with using liquid-crystal polarization optics for precise polarimetry is the lack of an inherent calibration. Tests done as part of this work have shown the sensitivity of nematic-type liquid crystals to wavelength, and other tests indicate a temperature sensitivity, too. The calibration must consider the telescope effect too, since the telescope itself represents one of the major sources of polarimetric uncertainty. For the present proof concept, calibration curves were developed prior to the observations, and the telescope plus polarization analyzer calibration was derived using a self-consistent method (see November 1991). Magnetograms derived in this way give a good qualitative representation of the solar magnetic fields and provide a demonstration of the technique and of the usefulness of the liquid-crystal technology. A follow up study will implement a precise in-situ polarimetric calibration for both the LCP and the NSO/SP VTT using the techniques studied here. The most extensive part of this study has been the investigation of precise in-situ calibration, which I describe in Section 4 (November and Elmore 1987, November, 1988. Dunn et al. 1989. November 1989, 1992a, 1992b, 1992c, 1993).

2. DESIGN CONCEPT OF POLARIMETER/SPECTRAL ANALYZER

Ramsey (1971) presents a simple and naturally compensating magnetograph design based upon a Lyot filter set in one fixed tuning position. The design exploits the properties of the natural Lyot-filter transmission functions to provide a complete set of polarization and spectral samples which give independent magnetic-field information in each sample. By virtue of the fact that a Lyot element gives a Fourier channel spectrum passband, a Lyot filter provides a complete Fourier analysis of the spectral line. Others have used this feature as the basis of a Fourier tachometer for precise Doppler velocity measurement and pointed out many of the advantages (Beckers et al. 1975, Evans 1980. Brown 1980, November 1984). Ramsey's scheme is a generalization because it can provide a complete spectral Fourier analysis in each of the four Stokes polarization parameters.

The simplest design of a Lyot element consists of a polarizer, followed by a birefringent crystal, followed by a second polarizer. The element gives a sinusoidal transmission function in wavelength whose spectral period is inversely proportional to the thickness of the birefringent crystal. Tuning of the element in wavelength or shifting the sinusoidal transmission function can be affected most simply by varying the effective optical thickness or retardance of the crystal by a small amount. By stacking Lyot elements in series

each with two times the thickness of the previous, we obtain a transmission function which is the product of sinusoids. The result is the single Lyot passband function illustrated in Figure 1.

Lyot Filter Design

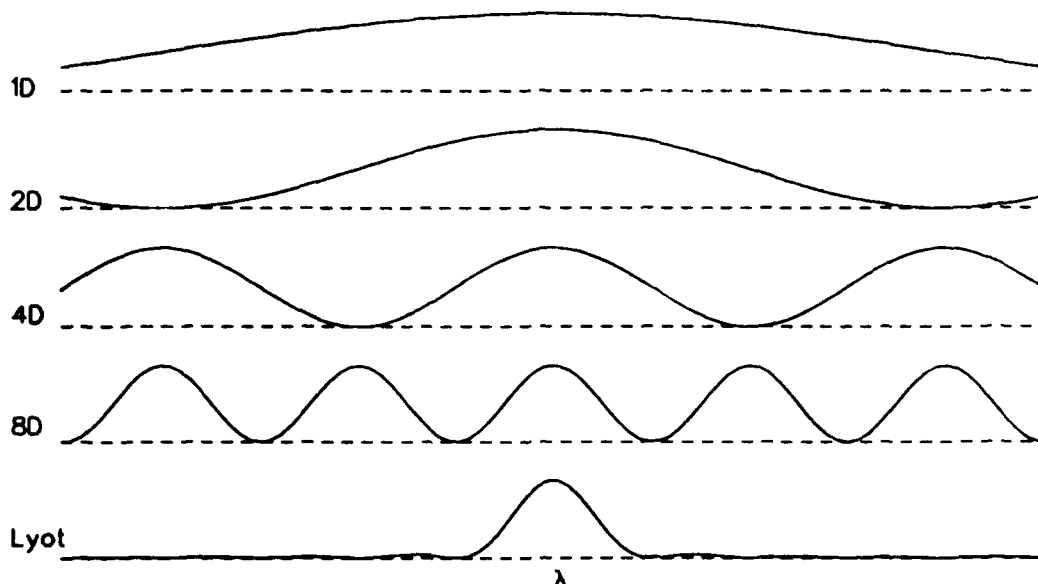


Figure 1: Lyot Filter Design. The spectral passbands are shown in wavelength λ for Lyot elements having thicknesses 1D, 2D, 4D, and 8D. The product gives the single Lyot passband function shown at the bottom.

By shifting the last Lyot element in the series, i.e. 8D, in phase with respect to the other elements, it is possible to obtain alternate transmission functions. Figure 2 shows four of these labeled T_+ , T_- , T_R , and T_B which are functions of the wavelength. T_+ is the normal Lyot filter transmission function. T_- is the transmission function for the last element detuned by 90° . Both of these are simultaneously available at the exit of the filter by using a polarizing beam splitter and studying both exit polarization states rather than extinguishing one (T_-) as is usual with Lyot filters. If a 45° spectral phase shift is introduced in the last Lyot element, then the two output signals T_R and T_B are obtained, similarly. The transmission difference functions $T_{even} = T_+ - T_-$ and $T_{odd} = T_R - T_B$ are shown in the bottom panel.

A full 2D image is obtained in each of the transmission functions T_\pm and T_{RB} since the Lyot system is a transmitting filter system. Then the difference transmission functions T_{even} and T_{odd} can be obtained by subtracting the T_+ and T_- images or the T_R and T_B images, respectively. The individual Stokes parameters can be imaged also by a modulation scheme. For example, for the input circularly polarized intensity $I + V$ the two output channels give $I + V$ in T_+ and T_- respectively. If we switch the input state to $I - V$ while simultaneously reversing the output channels, then we form the sum: $(I + V) \cdot T_+ + (I - V) \cdot T_-$, in one output channel and: $(I + V) \cdot T_- + (I - V) \cdot T_+$, in the other output channel. The difference gives directly: $V \cdot T_{even}$. This relationship is verified for general spectral integrals. It was Ramsey's observation that the resulting profile functions are very similar to the Zeeman profile functions produced by a magnetic field. Thus the system

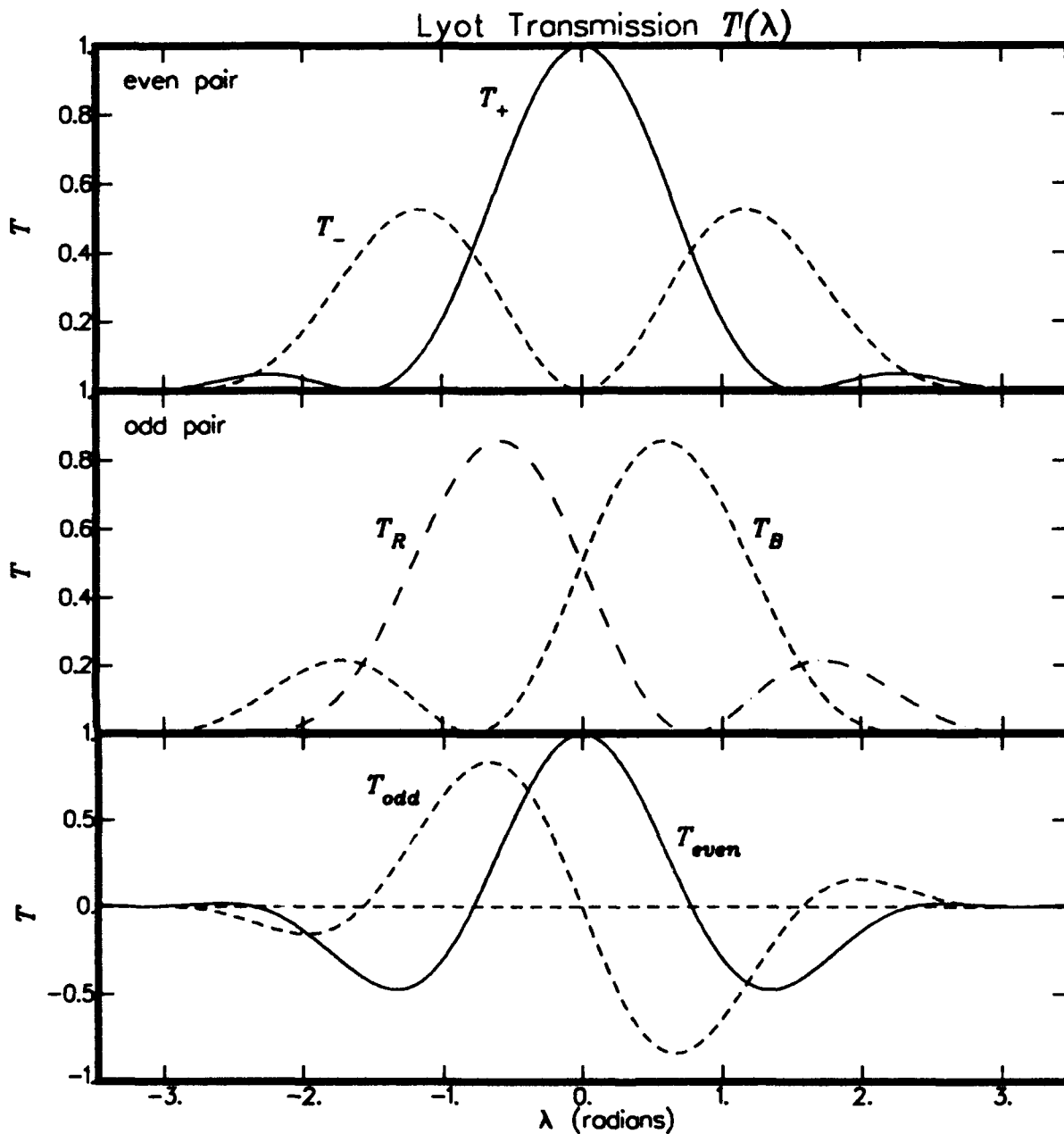


Figure 2: Lyot Spectral Transmission Functions. The spectral transmission functions for the two-channel Lyot system T_+ and with the last element detuned 90° T_- are shown in the upper panel. These two passband functions are simultaneously available using a polarizing beam splitter following the filter. The spectral transmission functions for the system detuned $\pm 45^\circ$, T_R and T_B , shown in the second panel are simultaneously available too. The difference functions $T_{\text{even}} = T_+ - T_-$ and $T_{\text{odd}} = T_R - T_B$ shown in the bottom panel represent the effective filter transmission function for the simultaneous difference signals.

separates directly the polarization/spectral components natural for the signal of interest in magnetic-field measurements.

The system consists of a polarimeter section which is placed before the NSO/SP Universal Birefringent Filter (UBF) and a spectral analyzer section which is placed immediately following the UBF in the light beam as shown in Figure 3. The polarimeter modulates the light at up to 31.5 kHz to give nearly simultaneous polarization and spectral images by temporal integration in two exit ccd channels. A sequence of 8 image pairs taken with combinations of settings in the polarimeter and spectral analyzer sections provides a complete polarization and spectral sample. The modulator control system provides multiple-frequency synchronous modulation of fast ferro-electric and slower tunable nematic liquid crystals, for use with normal ccds or for use with video. The eight experiment modes are specified by tuning the elements in the Liquid Crystal Polarimeter in Table 2.1.

Liquid Crystal Polarimeter w UBF

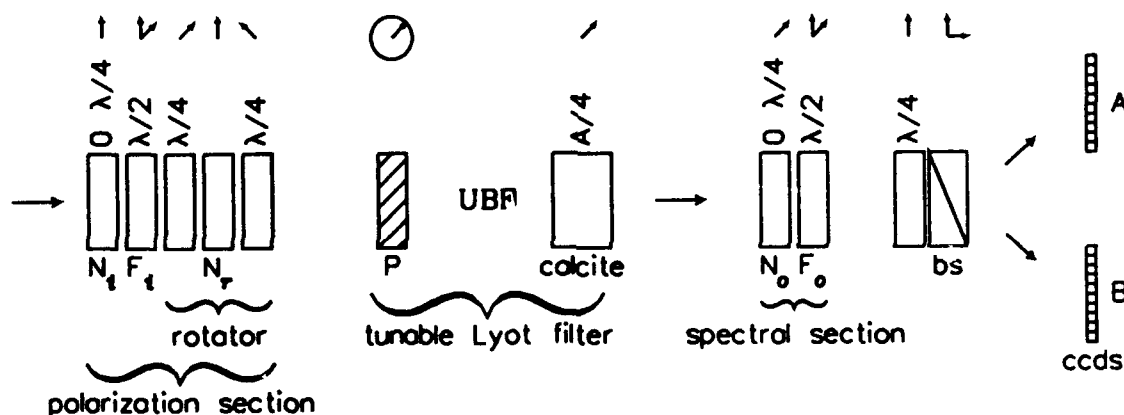


Figure 3: Schematic Design of Liquid Crystal Polarimeter with Universal Birefringent Filter. The combined LCP and UBF optical arrangement is shown. Each element is labeled according to type: N for nematic liquid crystal, F for ferro-electric liquid crystal, P for polarizer, bs for polarizing beam splitter, and no label for fixed wave plates. The polarimetric activity is given above each device with vectors showing the orientation(s) of its principle axis in the beam from the upward direction. The entrance polarization analyzer section can be set to give successive extinction and transmission of any single Stokes state. It contains a solid-state linear-polarization rotator section which is set to match the orientation of the entrance polarizer to the UBF. The exit spectral analyzer section switches the spectral transmission function between the two output channels A and B.

The control electronics synchronously operates all of the liquid crystals with DC analog input for setting the voltage in each nematic and with three control bits for each ferro-electric. All of the nematics are modulated at a high frequency (5 kHz) at the specified voltage amplitude. The three bits for the ferroelectrics represent high frequency on, 30 Hz frequency on, and switch phase. The frequencies are logically added, e.g. high frequency

modes:	N_i	F_i	N_r	N_o	F_o
I_{even} :	0	fast rate	rot	0	ccd rate
I_{odd} :	0	fast rate	rot	$\lambda/4$	ccd rate
Q_{even} :	0	fast rate	rot	0	fast+ccd rate
Q_{odd} :	0	fast rate	rot	$\lambda/4$	fast+ccd rate
U_{even} :	0	- fast rate	$\lambda/4$ +rot	0	fast+ccd rate
U_{odd} :	0	- fast rate	$\lambda/4$ +rot	$\lambda/4$	fast+ccd rate
V_{even} :	$\lambda/4$	fast rate	rot	0	fast+ccd rate
V_{odd} :	$\lambda/4$	fast rate	rot	$\lambda/4$	fast+ccd rate

Table 2.1: LCP Operating Modes and Timing. The retardance values and modulation frequencies are shown for each of the five liquid crystals for each of the 8 basic modes of the experiment. The liquid crystal N_i and F_i correspond to the first two elements in the polarization section of Figure 3; N_r is in the rotator; N_o and F_o are after the UBF in the spectral section and control output through the beam splitter. The retardance rot for N_r refers to a variable value that is set according to the orientation of the entrance polarizer to the UBF which changes with the spectral line. F_i and F_o run in sync at a fast frequency which is an integer fraction of the base rate 31.5 kHz, two times the video horizontal-line frequency.

plus 30 Hz implies that the ferroelectric is modulated at the high frequency and is switched in its phase at the 30 Hz rate. All of the ferroelectrics are modulated in phase based upon external sync signals. The 30 Hz external sync is common to all the VTT video systems to guarantee synchronous camera operation. The high frequency is set to be a integer fraction of two times the video horizontal-line rate, 31.5 kHz. This frequency was chosen so that it is possible to obtain equal exposures of the two signals in each output channel in one video frame. The control signals are latched in sync with the ccd rate to avoid the need for critical event timing in the host computer. The ferroelectrics automatically switch in phase after 3 seconds if the first two bits are not set and the third bit is not changed, because material damage occurs if they are not cycled.

The various combinations permit setting of specific experiments in each exposure or video frame. If the high frequency bit alone is set for the input ferroelectric F_i and not for the output ferroelectric, F_o , as in the I_{even} and I_{odd} experiments in Table 2.1, then modulation of the input polarization occurs summing two polarization states, e.g. $I + Q$ plus $I - Q$, to give just the unpolarized I . The slow switching of F_o at the ccd rate is accomplished by setting the 30 Hz bit for video or by switching the phase change bit between frames for slow-readout ccds. This switching interchanges the output spectral channels in successive cycles which is useful for automatic gain/dc correction in the ccds as we discuss below. In all of the polarized-light operating modes: Q_{even} , Q_{odd} , U_{even} , U_{odd} , V_{even} , and V_{odd} , both ferroelectrics F_i and F_o are modulated at the high rate. In addition F_o is also modulated at the ccd rate to change the phase of the output spectral channel in successive ccd cycles.

Each of the 8 experiments are always performed at least twice in sequence, reversing the sense of the detectors for the repeat. A summed difference signal from the two experiments then subtracts the constant dark current from the two signals. Ratios of differences

give the relevant physical parameters as we discuss in the next section, so the process leads to an automatic gain correction also. There is a small seeing-gain cross talk that occurs if the seeing is of differing quality in the repeat. An approximate calibration procedure avoids this seeing-gain cross talk. For now, the observations were obtained in the eight experiment modes shown in Table 2.1, each executed twice for a total of 16 ccd image pairs per set.

The nematic crystals were each calibrated on the bench as a function of color and temperature. Figure 4 shows examples of the response functions. Each nematic liquid crystal has a different response function, and for purposes of the experiment, the voltage for a desired retardance was given by direct interpolation in the smoothed response curves.

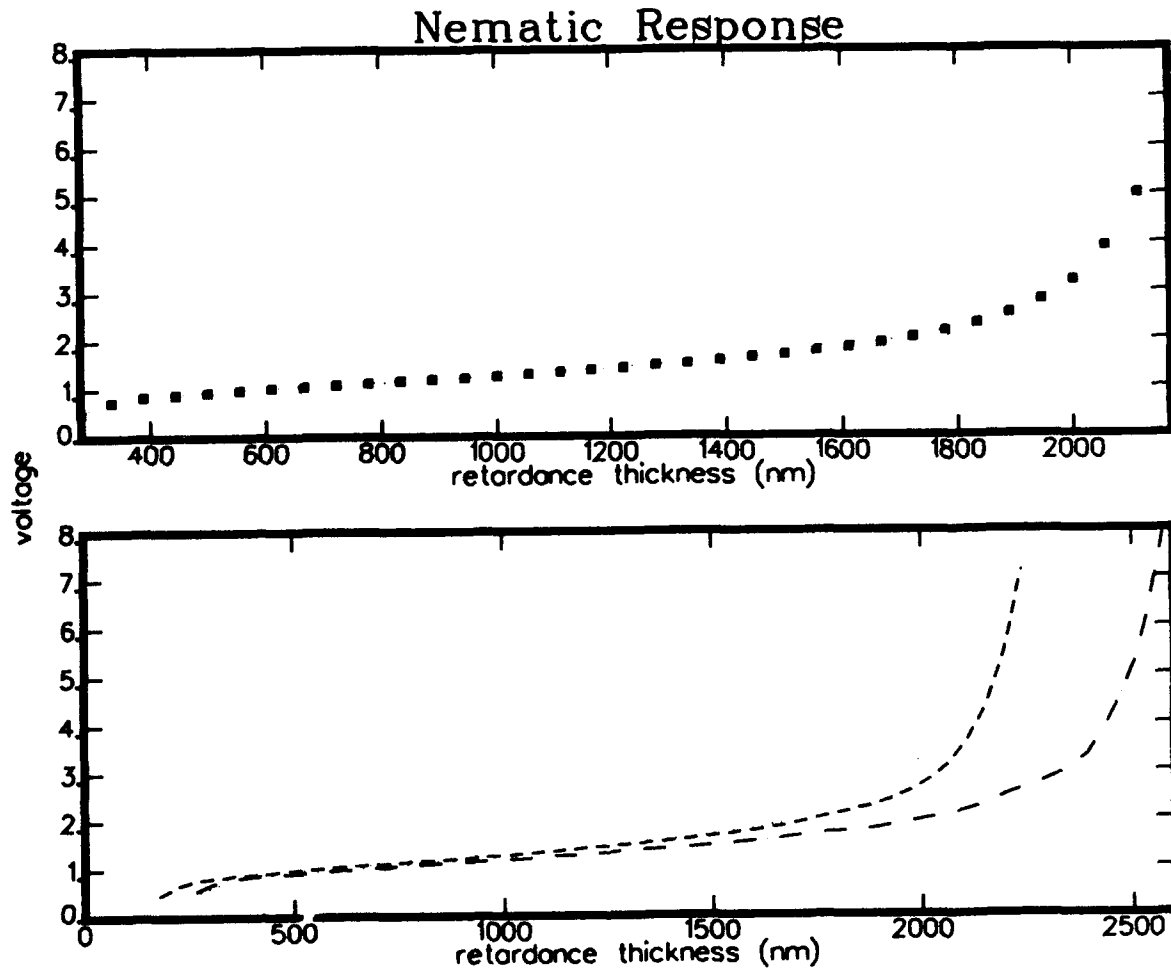


Figure 4: Nematic Response Voltage as a Function of Retardance. The upper panel shows the actual measured values and the smoothed curve through the measurements for red illumination, $6670\text{\AA} \pm 50\text{\AA}$. The lower panel shows smoothed response curves for the same nematic liquid crystal for red (dotted), $6670\text{\AA} \pm 50\text{\AA}$, for green (dashed), $5380\text{\AA} \pm 50\text{\AA}$, and for blue (dash-dot), $4560\text{\AA} \pm 50\text{\AA}$, illumination.

3. EXPERIMENTAL RESULTS

The Liquid Crystal Polarimeter (LCP) was assembled and tested at the NSO/SP Vacuum Tower Telescope during an observing run March 9-16, 1992. The system can be operated in many spectral lines using the general tuning property of the Sacramento Peak/Universal Birefringent Filter (UBF) (4000Å to 7000Å). The UBF is a mechanically tuned Lyot-type birefringent filter with a passband of 0.24Å at 6563Å. The passband goes like λ^2 , so it is a 0.155Å passband filter at 5172Å MgB.

The LCP system provided initial vector magnetograms in 4 lines: MgB 5173Å, CaI 6103Å, FeI 5247.8Å, and FeI 5250.2Å. Figures 5 and 6 show the polarization maps for MgB derived from one complete set of samples. The spectrally even polarization images are plotted on a range of $\pm 4\%$ in Figure 5 compared to the unpolarized line strength. There is no evidence of systematic effects due to the gain table of the chips which individually showed fringes and bad pixels. Seeing misregistration effects are not evident. Seeing residuals are common to all other magnetogram systems which employ sequential acquisition of the conjugate polarization components with one detector. Thus the two detection method is advantageous in two ways.

The signal to noise is rather low, characteristic of the transverse magnetic field signal. This signal to noise is consistent with the photon statistics for the 4 ccd images that go into each image. The spectrally odd polarization images from Figure 6 show less noise characteristic of the higher signal for the longitudinal magnetic field.

We might expect that the V_{even}/I_{even} , Q_{odd}/I_{even} , and U_{odd}/I_{even} signals should be zero. The transverse magnetic field produces an even spectral component that is polarized only in Q and U , and the longitudinal magnetic field produces an odd spectral component that is polarized only in V for the normal Zeeman effect. However, Doppler velocity shifts the line-center position with respect to the filter passband and leads to approximately 5% crosstalk between the spectrally odd and even components for a given polarization state. The effect can be removed exactly because the I_{odd}/I_{even} map gives the line center position at each pixel in the image. The Lyot filter natural profile function, Figure 2, provides a complete spectral sample which allows precise spectral shifting of the measurement (November 1984).

The second source of cross talk between the components is caused by the polarization effect of the telescope. The telescope has oblique reflections and stressed vacuum windows which introduce partial absorption and polarization retardation. Thus there is mapping between the polarization components in the even and in the odd images (see November 1988, 1989). This effect is large (30%-50%) and can be removed, in principle, by applying the inverse matrix of the telescope.

It is a convenient property of the Sacramento Peak Vacuum Tower Telescope that the linear polarization state is not rotated by more than 3.5° . Figure 7 shows an actual measurement made during the course of one day by rotating a large sheet polarizer placed over the entrance window while making polarization measurements at the telescope exit port. Thus the linear polarization direction measured by the polarimeter in the solar image must be the correct linear polarization direction on the sun. We therefore take Q_{even}/I_{even} and U_{even}/I_{even} as representative of the transverse field. The V_{even}/I_{even} component must be mainly a linear combination of the two mapped from the telescope matrix.

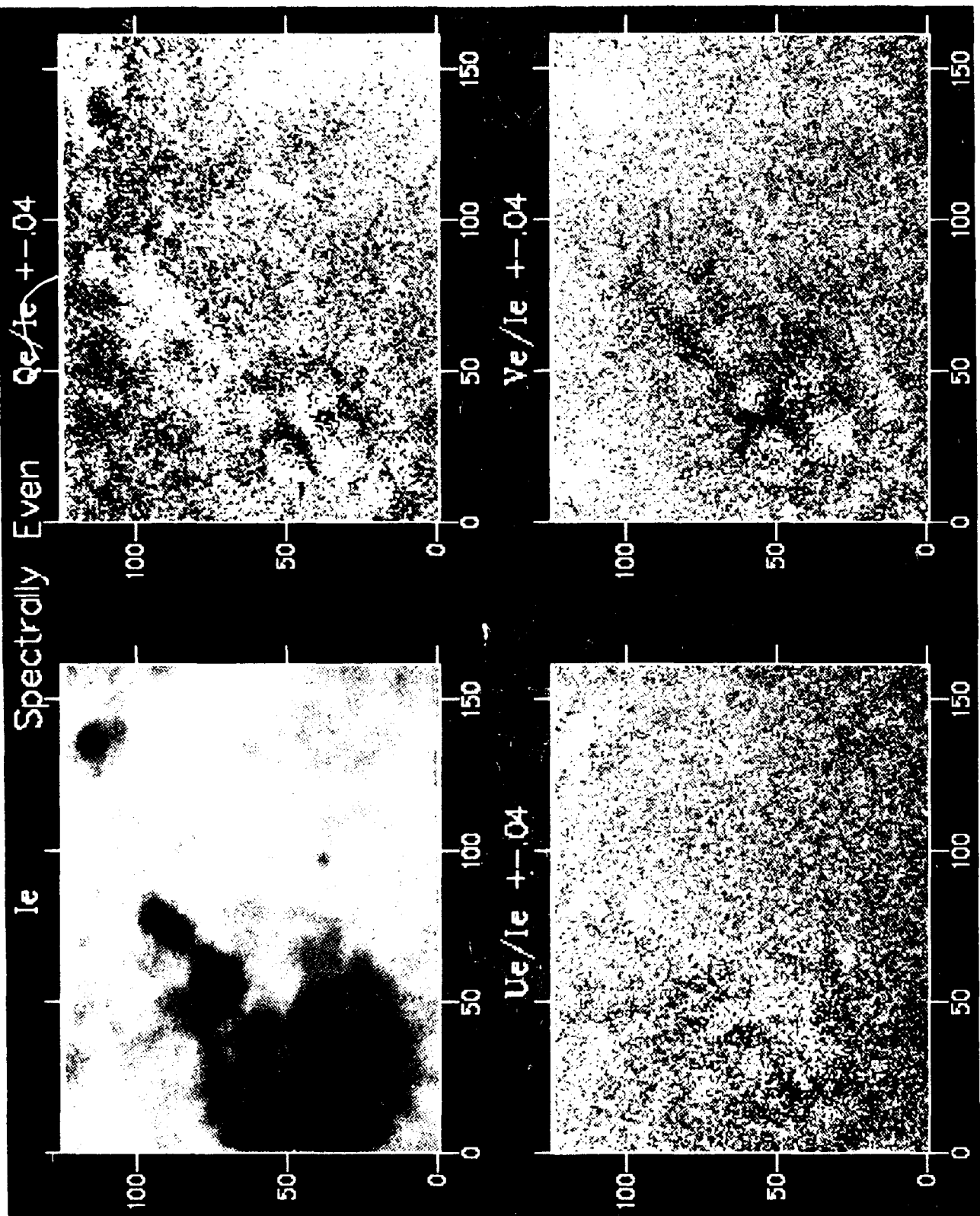


Figure 5: Spectrally Even Polarization Images for MgB of an Active Region. The I Stokes signal times the even spectral transmission function T_{even} . I_{even} is shown in the 160×120 arcsec field of an active region. I_{even} is a measure of the line strength. The relative even Stokes signals Q_{even}/I_{even} , U_{even}/I_{even} , V_{even}/I_{even} are shown on a scale of $\pm 4\%$. The even Stokes signals contain the transverse magnetic flux and direction.

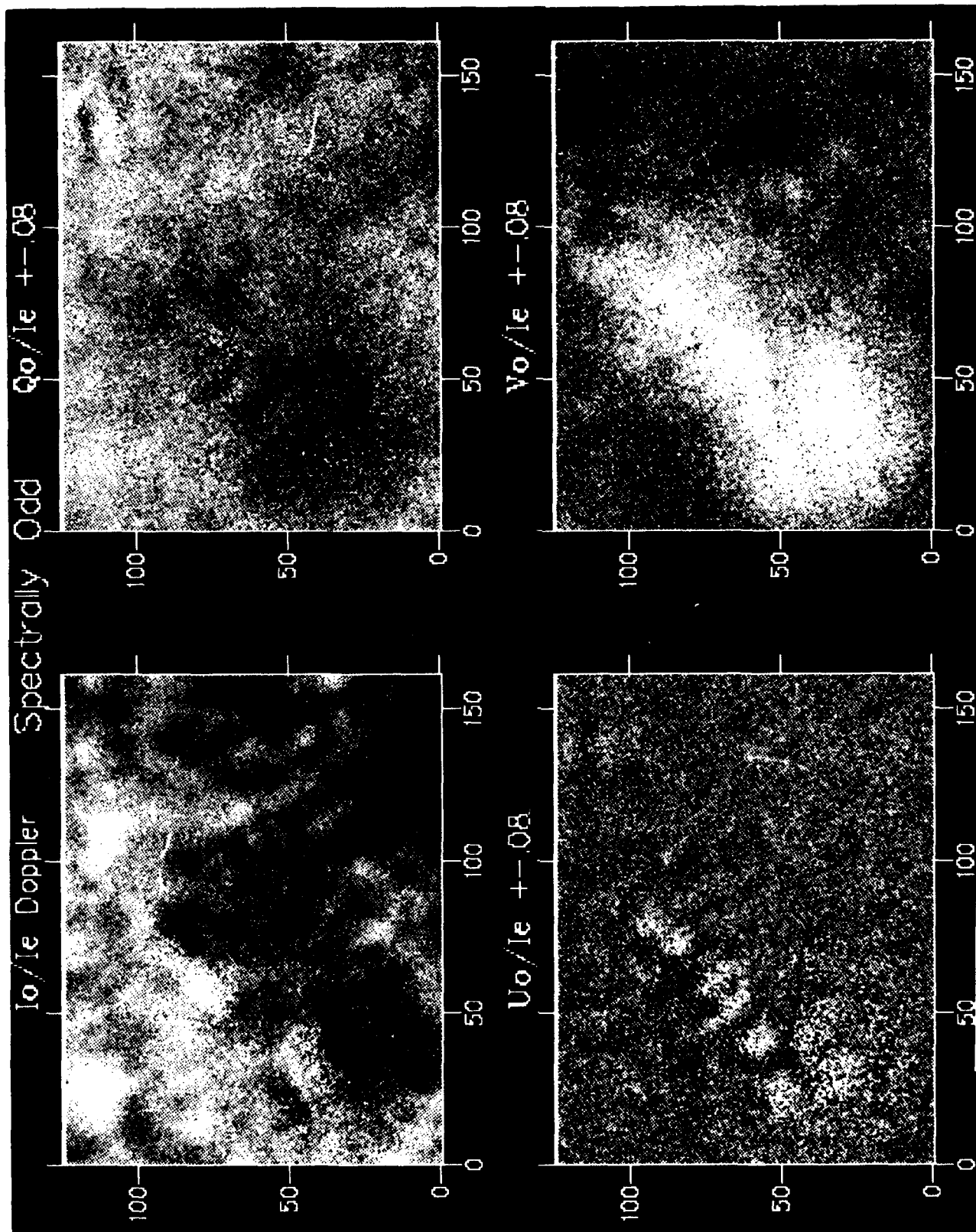


Figure 6: Spectrally Odd Polarization Images for MgB . The normalized odd Stokes signal, I_{odd}/I_{even} , is a measure of the line shift or Doppler velocity. The relative odd Stokes signals Q_{odd}/I_{even} , U_{odd}/I_{even} , V_{odd}/I_{even} are shown on a scale of $\pm 8\%$. The odd Stokes signals give a measure of the longitudinal magnetic flux.

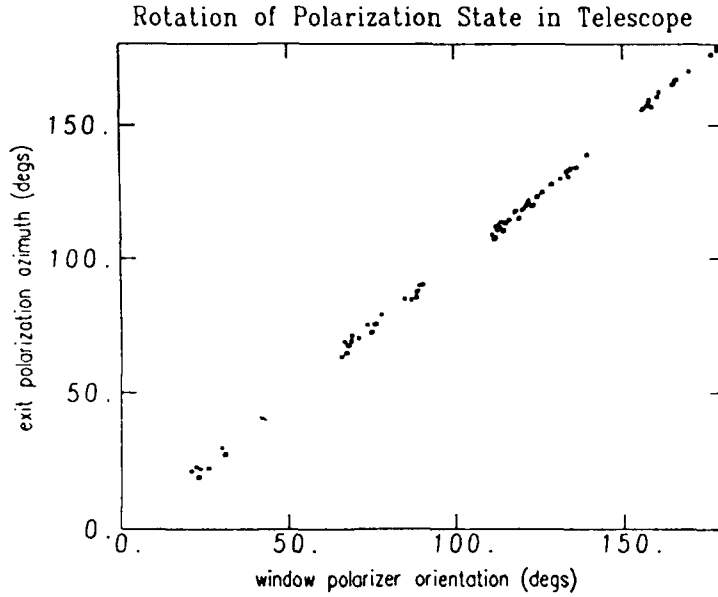


Figure 7: Rotation of Polarization Azimuth in the SP/VTT. The measured output linear polarization direction is plotted as a function of the linear polarization direction at the entrance of the SP/VTT. The measurement was made by rotating a large sheet polarizer in front of the telescope entrance window during the course of one day while making measurements at the exit port (see November and Elmore 1987). Though the telescope has approximately 30° retardation effect which changes during the day, the linear polarization direction is preserved within 3.5° . The effect can be understood as a natural statistical property for an optical system consisting of multiple weak elements which each have linear polarization principle axes (see November 1989).

The longitudinal field produces principally a V polarized odd state which is mapped partially into Q_{odd}/I_{even} and U_{odd}/I_{even} by the telescope. Therefore the V_{odd}/I_{even} signal alone can be taken as representative of the longitudinal magnetic field. In Figure 8, contours of V_{odd}/I_{even} are shown plotted on the line strength I_{even} image with vectors showing the amplitude and direction from the Q_{even}/I_{even} and U_{even}/I_{even} images. Figure 8 is therefore the vector magnetogram which depicts the longitudinal and transverse magnetic flux.

In addition there is some evidence for a variation of the polarization effect over the field of view. This effect can be seen in Figure 5 for Q_{even}/I_{even} as a positive (light) enhancement along the lower right side of the image. Field of view polarization effects were not considered in the present analysis. More exact methods will be employed in a follow up study using the methodology for in-situ calibration described in the next section.

The Doppler velocity is accurately represented in I_{odd}/I_{even} with a small systematic correction due to line width/blocking filter cross talk (November 1984). The line strength and continuum intensity are contained in the I_{even} image and sum images $I_+ + I_-$. With multiple spectral lines from the same multiplet it is possible to separate the magnetic-field strength and partial filling factor using well-known techniques. Multiple spectral lines differing in height of formation provide height resolution of the physical parameters. Fourier

Vector Magnetogram with Liquid Crystal Polarimeter

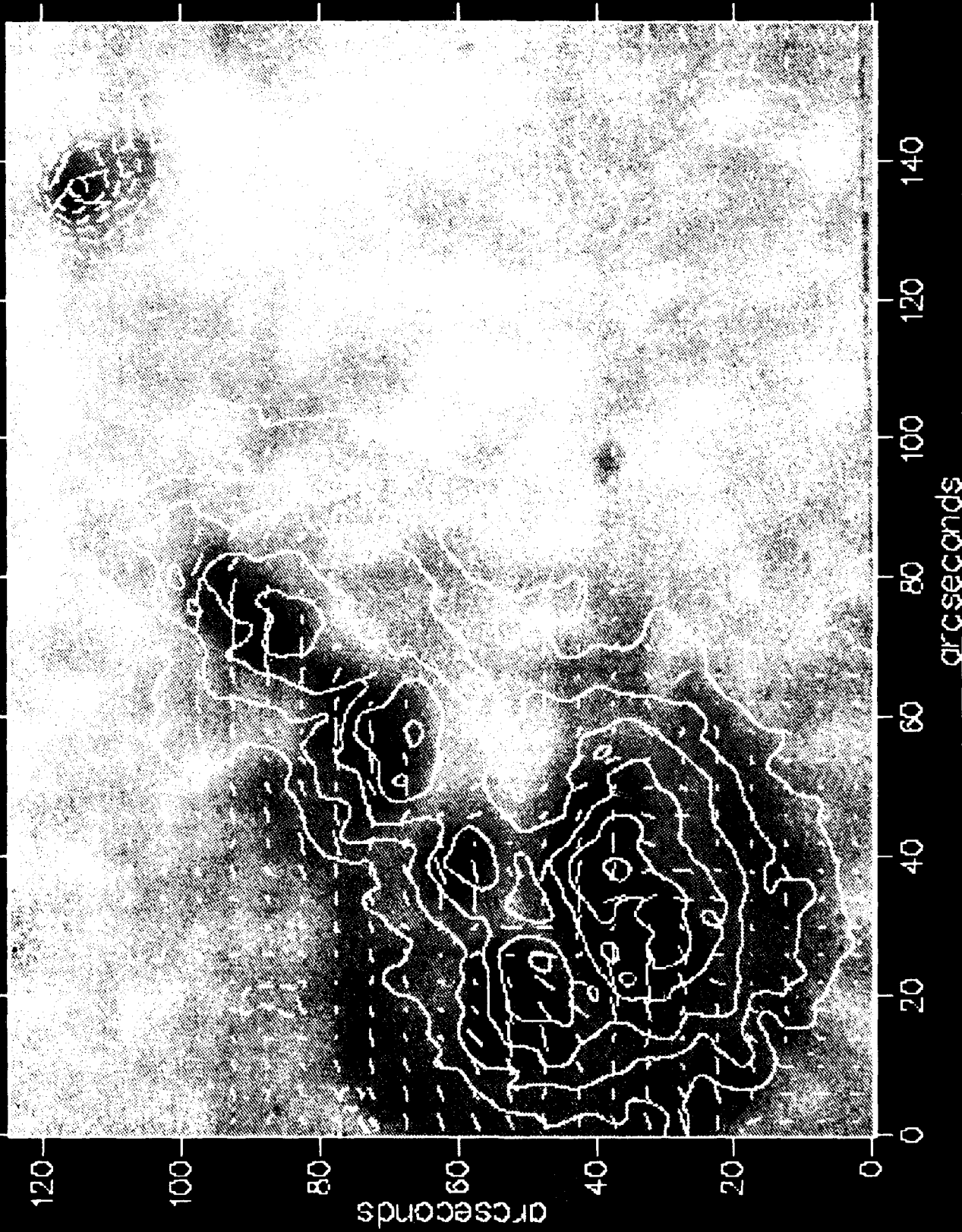


Figure 8: Vector Magnetogram acquired with Liquid Crystal Polarimeter. Equal contours of longitudinal magnetic flux are shown plotted over the relative line strength in half tones. solid contours for positive longitudinal field and dashed for negative. Vectors showing the linear polarization direction and amplitude are superimposed.

spectral parameters are known to be relatively insensitive to line shape (Brown 1980, Evans 1980, November 1984), and so this system may provide measured parameters that are relatively insensitive to the atmospheric model. Sensitivity of the measured parameters to the atmospheric model is a large effect in other magnetographs which spectrally undersample the line-profile function. A follow up study will investigate the detailed line formation properties for a number of solar lines sampled by this type of Fourier spectral analysis.

Initial tests showed the feasibility for studying electric fields using the same system. The filter was run in the Balmer lines $H\alpha$, $H\beta$, $H\gamma$, $H\delta$ with the LCP in an exploratory test. Ratios of parameters in different Hydrogenic lines provide a measure of the electric-field strength through the Stark effect.

4. IN-SITU CALIBRATION

The present system provides very good magnetic-field vector-component separation because of the good spectral discrimination inherent in this complete Fourier sample. Thus it was possible to apply self-consistent methods in the present analysis. A more exact methodology shows the power of using spectral information alone to discriminate between telescope and solar polarization effects (see November 1991).

However, it is better that a calibration procedure use separate information to determine the optical-system polarization transformation separate from the solar observation. It is preferable too, that it be done in situ to consider multiple-element alignment effects and the possibility of slow variations with time.

Calibration in situ is performed by inserting known polarization sources into the optical system and measuring the modified polarization states at the exit. We think of the classical Mueller representation where four independent polarization states taken as input with measurements at the output determine the Mueller matrix for the device. However, the classical Mueller matrix derived in this way suffers from several defects: (1) Naturally precise circularly polarized sources are not available and an independent polarized V state can not be obtained directly. Retardation is required to produce a circularly polarized state, but most retardation sources are wavelength, temperature, and optical alignment sensitive (see November 1992b, 1992c, 1993). (2) The Mueller representation is an over-specification which does not uniquely decompose into physical device parameters. (3) Mueller matrices can be derived numerically that give nonphysical solutions, corresponding to the creation of polarization which can lead to light states that are more than 100% polarized in applying the Mueller matrix.

It is possible to obtain the Jones matrix or an enhanced form including isotropic depolarization which accurately represents optical imaging systems (see November 1989, 1992a). These solutions have the advantage that they are determined using three independent polarization sources thus precluding the need for a circularly polarized source. It is possible to obtain inherently precise wide-field linear-polarization sources using Glan-Thompson, Wollaston, or Rochon prisms which are natural linear polarizers based upon the properties of optically nonactive crystals. Rotation of the linear polarizer is sufficient to obtain three independent polarization sources.

This methodology is the basis for my proposal for precise in-situ calibration of the telescope and Liquid Crystal Polarimeter. Special hardware will affect the insertion of

a precisely rotatable linear polarizer before the telescope. Rotation of a linear polarizer that covers a small portion of the aperture can give a single matrix for the optical system. Spatial nonuniformities in the solution can be calibrated independently using magnetic images made in quiet sun, because the important effects are due to the cross talk from unpolarized into polarized components.

The telescope has the difficulty that it has a systematically changing matrix due to the changing pointing during the day. The reflection angles change and correspondingly the individual device matrices change, so that the serial product matrix that represents the whole system changes. I showed that extrapolation of the Jones matrix for a serial-element polarized light system of n rotating elements can be performed exactly, given n matrix determinations of the whole system with independent element angles (see November 1988, 1989). Thus, the SP/VTT with 3 independent rotating optical elements requires 3 matrix determinations to infer the matrix for the system for all possible orientations of the optical elements. A few calibrations done during the day can be applied at all times during the day or to adjacent day's observations. This solution generalizes to depolarizing systems as well (November 1992d).

5. CONCLUSION

The Liquid Crystal Polarimeter demonstrates the possibility for solid-state imaging of solar magnetic fields. The natural profile function for the Lyot filter provides an ideal spectral mask that allows the independent polarization/spectral components to be obtained in a minimum of measurements without moving parts. The system provides for almost simultaneous imaging in conjugate components using the rapid switching capability of ferro-electric liquid crystals to give difference images that are unaffected by atmospheric seeing. The difference images provide complete magnetic-field information as we demonstrated here, or can be used for imaging other polarization parameters like electric field or impact polarization. The solid-state design combined with the natural passband characteristics for the Lyot filter provide a considerable simplification to previous designs and with greatly improved reliability. With proper polarimetric and field-strength calibration, the system should provide an inherently high measurement precision.

The fast tuning system operating in the relatively broad passband gives the possibility for video imaging. Though the magnetogram shown here took 30 seconds to obtain, the same signal is available in about 1/2 second. The loss due to the readout time of the detector could be eliminated by using video. Hardware is now becoming available for handling the data rate and we anticipate implementing a fast video acquisition system soon. With this upgrade the present system will have a maximum polarimetric sensitivity and speed, for studying weak fields, rapidly changing phenomena, and high-resolution morphology.

Although polarimetric calibration of liquid crystal elements is necessary, in-situ methods for automatic calibration have been developed which will permit independently verified polarimetric precision. The calibration method is an alternative to the well known Mueller matrix method. The device is characterized by a restricted form that excludes nonisotropic depolarization effects, with is a representation ideally suited for imaging optical systems. The method provides a general polarization determination with reference only to a rotating linear polarizer and does not rely upon given circularly polarized sources.

The particular calibration problem for a telescope is that it contains multiple rotating elements in series which are continuously changing in time. A general extrapolation formula was developed for serial-element systems which allows interpolation between telescope matrix measurements in a single day or the application of measurements made on one day to adjacent observing days.

An improved system could be obtained by combining the Liquid Crystal Polarimeter with a solid-state tuning Lyot filter. Such a system would give the possibility for multi-wavelength differential photometry and for more detailed spectral line analyses.

ACKNOWLEDGEMENTS

This work was motivated by Harry Ramsey's original investigations into liquid crystals. The design concept profited from many useful discussions with him. Fritz Stauffer provided the software computer interface for synchronous ccd camera control. The reported observations were carried out at the SP/VTT with the help of the National Solar Observatory observing staff: R. Mann, E. Stratton, and S. Hegwer.

REFERENCES

- Beckers, J.M., Dickson, L., and Joyce, R.S., 1975. "A Fully Tunable Lyot-Ohman Filter". AFCRL-TR-75-0090, Air Force Cambridge Research Lab., Office of Aerospace Research, United States Air Force. ADA011599
- Brown, T.M., 1980, "The Fourier Tachometer: Principles of Operation and Current Status", *Solar Instrumentation: What's Next*, Proceedings of the National Solar Observatory/Sacramento Peak Workshop, ed. R. Dunn, 150-154.
- Dunn, R.B., November, L.J., Colley, S.A., Streander, G.W., 1989. "The National Solar Observatory Polarimeter". *Optical Engineering* **28**, 126-130.
- Evans, J.W., 1980, "The Fourier Tachometer: A Solid Polarizing Interferometer". *Solar Instrumentation: What's Next*, Proceedings of the National Solar Observatory/Sacramento Peak Workshop, ed. R. Dunn, 155-169.
- November, L.J., 1984, "Radial Velocity Measurements of the Sun Made with a Birefringent Filter". *Small-Scale Dynamical Processes in Quiet Stellar Atmospheres*, Proceedings of the National Solar Observatory/ Sacramento Peak Workshop, ed. S. Keil, 74-87.
- November, L.J., and Elmore, D.E., 1987. "Measurement of the polarization properties of the NSO/Sunspot Vacuum Tower Telescope", *B.A.A.S.*
- November, L.J., 1988, "Measurement of a multiple component serial device of partial polarizing and retarding elements", *Polarization Considerations for Optical Systems*, ed. R. Chipman, SPIE 891, 91-102.
- November, L.J., 1989, "Determination of the Jones Matrix for the Sacramento Peak Vacuum Tower Telescope", *Optical Engineering* **28**, 107-113.
- November, L.J., 1991, "Using the Zeeman Spectral-Polarization Symmetry for Telescope Calibration", *Solar Polarimetry*, Proceedings of the Eleventh National Solar Observatory/Sacramento Peak Workshop, ed. L. November.

- November, L.J., 1992a, "Recovery of the matrix operators in the similarity and congruency transformations: applications in polarimetry", *Jour. Op. Soc. Am. A*, accepted.
- November, L.J., 1992b, "Exploiting spatial transformations of the light state for precise polarimetry", *Polarization Analysis and Measurement*, ed. D. Goldstein, R. Chipman, SPIE 1746.
- November, L.J., 1992c, "The indistinguishability of geometric and polarization transformations", *Optical Engineering*, in preparation.
- November, L.J., 1992d, "Decomposition of Multiple Element Serial Polarized-Light Systems", *Jour. Op. Soc. Am. A*, in preparation.
- November, L.J., 1993, "In-Situ Calibration for Precise Polarimetry", *Trends in Optical Engineering*, ed. J. Mehon, invited review in preparation.
- Ramsey, H.E., 1971, "Use of a Birefringent Element to Separate Magnetic Polarity", *Solar Physics* **21**, 54-56.